



Research article

A mathematical model between keystone species: Bears, salmon and vegetation

Christopher Middlebrook and Xiaoying Wang*

Department of Mathematics, Trent University, Peterborough, ON K9L 0G2, Canada

* **Correspondence:** Email: xiaoyingwang@trentu.ca.

Abstract: We study an ecosystem of three keystone species: salmon, bears and vegetation. Bears consume salmon and vegetation for energy and nutrient intake, but the food quality differs significantly due to the nutritional level difference between salmon and vegetation. We propose a stoichiometric predator-prey model that not only tracks the energy flow from one trophic level to another but also nutrient recycling in the system. Analytical results show that bears may coexist with salmon and vegetation at a steady state, but the abundance of salmon may differ under different regimes. Numerical simulations reveal that a smaller vegetation growth rate may drive the vegetation population to extinction, whereas a large vegetation growth rate may drive the salmon population to extinction. Moreover, a large vegetation growth rate may stabilize the system where the bear, salmon and vegetation populations oscillate periodically.

Keywords: stoichiometry; predator-prey model; nitrogen recycling; stability; coexistence

1. Introduction

A keystone species is one on which other species in the ecosystem largely depend. So much so that if removed there are drastic effects on the ecosystem [1]. Bears, salmon and vegetation are unique in an ecosystem because all three are keystone species dependent on one another [2]. In this ecosystem, salmon and vegetation are both food resources for bears, but the food quality differs significantly.

Salmon are much more nutrient-rich compared to vegetation, i.e., the nitrogen/phosphorous etc. concentration within salmon's bodies is much higher compared to vegetation. However, salmon must maintain homeostasis of element concentration within the body so that they must excrete excessive nutrients into the environment if the element concentration exceeds a threshold. On the other side, vegetation is less nutrient-rich but can absorb the remaining nutrient in the environment so the nutrient level within vegetation may differ significantly over time at an order of different magnitude [3–5].

Bears share common characteristics with salmon where bears are also nutrient-rich but must main-

tain a homeostasis of element concentration within their bodies [3–5]. When consuming poor-quality food where the element concentration is low, the energy conversion from food consumption to the bear biomass cannot be maximized. In the bear-salmon-vegetation ecosystem, salmon is good-quality food, whereas vegetation is poor-quality food. Therefore, when studying the bear-salmon-vegetation ecosystem, it is important to devise a model that depicts not only the energy transfer but also the nutrient flow between trophic levels.

One of the well-known models that study stoichiometric population dynamics is the one proposed by Loladze and Kuang [6]. The model builds on classical predator-prey models of one consumer and one food resource but incorporates a single limiting element phosphorus into modeling to distinguish food quantity and food quality. Following [6], stoichiometric models have been studied extensively, see [7–13] for example. More recently, Phan, Elser and Kuang extended the previous producer-grazer model framework by including multiple shared limiting elements in the modeling [14]. The formulated model excludes the non-smoothness in the original stoichiometric model but replicates qualitatively similar dynamics in a wide range of parameters [14]. We follow the modeling framework of the aforementioned studies but extend the model to include a specific nutrient-rich food resource, which agrees with the bear-salmon-vegetation ecosystem. In particular, we choose nitrogen as the limiting element of the system because nitrogen is vital for all salmon, bears and vegetation.

We organize the paper in the following. In Section 2, we formulate a stoichiometric model of one consumer and two food resources, where one food resource is of good quality but the other food resource is of poor quality. In Section 3, we analyze the existence and local stability of the steady-state solutions. In Section 4, we conduct numerical simulations that confirm the analytical results. Moreover, numerical simulations also reveal interesting dynamics when certain parameters vary in a range. We end this paper in Section 5 with conclusions and discussions.

2. Model formulation

In the bear-salmon-vegetation ecosystem, salmon and vegetation are both food resources for bears but bears do not consume certain organs of salmon. Rather, bears leave salmon corpses around vegetation so that the vegetation absorbs any remaining nitrogen that ultimately contributes to the growth of its population. Moreover, bears and salmon are much more nutrient-rich compared to vegetation. However, salmon and bears must maintain homeostasis in nitrogen concentration within their bodies and excrete excessive nitrogen into the environment. Vegetation is less nutrient-rich but can absorb the remaining nitrogen in the environment so the nitrogen concentration in vegetation may vary at an order of different magnitude.

We first formulate a model that includes the energy transfer among trophic levels when nitrogen is abundant among all three species. Denote $S(t)$, $V(t)$, $B(t)$ by the salmon population density (measured in carbon per litre), the vegetation population density (measured in carbon per litre) and the bear population density (measured in carbon per litre) respectively. The model is

$$\begin{aligned} S'(t) &= \alpha S - f(S)B, \\ V'(t) &= \gamma V \left[1 - \frac{V}{K} \right] - g(V)B + \epsilon f(S)B + \psi B, \\ B'(t) &= e_1 f(S)B + e_2 g(V)B - \lambda B, \end{aligned} \tag{2.1}$$

where α is the growth rate of the salmon population, $f(S)$ is the consumption rate of salmon by the bear, γ is the intrinsic growth rate of the vegetation, K is the carrying capacity of the environment, $g(V)$ represents the consumption rate of vegetation by the bear, e_1 and e_2 are the energy conversion rate from the consumption of the salmon and the vegetation respectively and λ is the natural death rate of the bear. In (2.1), ϵ represents the rate of contribution to the vegetation growth due to the element recycling from the nearby salmon corpses left by bears. Furthermore, the bears produce excrement after digesting the salmon, which provides another source for vegetation to absorb the nitrogen, which contributes positively to vegetation growth at a rate of ψ [2].

The above model (2.1) assumes a linear growth rate for the salmon and a logistic growth for the vegetation. Having spent most of their lives feeding and growing at sea, salmon return to spawn and die. Salmon return to their natal streams carrying marine-derived nutrients in their body tissues. In particular, adult salmon are rich in nitrogen [2]. Salmon do not compete for resources which implies it is safe to assume a linear growth rate of γ . Vegetation, on the other hand, competes for resources limited by solar energy and follows a logistic growth rate. However, the vegetation population is not only limited by light but is also regulated by nitrogen concentration.

Because of the homeostasis of bears and salmon, we can safely assume that the N: C (nitrogen: carbon) ratio within bears and salmon are θ_1 and θ_2 respectively. It follows that the remaining nitrogen in the environment is $N - \theta_1 B(t) - \theta_2 S(t)$. Moreover, following [6], we assume that the N: C (nitrogen: carbon) ratio within the vegetation never falls below a level N_V . Combining the assumptions, we obtain another carrying capacity of the vegetation limited by nitrogen as

$$\frac{N - \theta_1 B(t) - \theta_2 S(t)}{N_V}.$$

Together with the carrying capacity limited by solar energy, we obtain an improved carrying capacity for the vegetation population

$$\min \left\{ K, \frac{N - \theta_1 B(t) - \theta_2 S(t)}{N_V} \right\}.$$

Following [6], we assume that all of the nitrogen within the system gets recycled immediately and there is no pool of free nitrogen in the environment.

It follows that the N: C ratio in vegetation is

$$\frac{N - \theta_1 B(t) - \theta_2 S(t)}{V(t)}.$$

Vegetation serves as good-quality food for bears if

$$\frac{N - \theta_1 B(t) - \theta_2 S(t)}{V(t)} \geq \theta_1,$$

or equivalently

$$\frac{N - \theta_1 B(t) - \theta_2 S(t)}{\theta_1 V(t)} \geq 1,$$

and is poor-quality food otherwise. If vegetation is good-quality food, the biomass conversion from the vegetation to the bear follows the maximum energy intake e_2 . However, if vegetation is poor-quality food, the biomass conversion is reduced by a ratio

$$\frac{N - \theta_1 B(t) - \theta_2 S(t)}{\theta_1 V(t)}.$$

Hence, biomass conversion efficiency is not a constant but depends on both energetic and nutrient limitations. Note that we can assume that salmon is a good-quality food source for bears since salmon is nutrient-rich. Following [6], we formulate the biomass conversion from vegetation consumption as

$$e_2 \min \left\{ 1, \frac{N - \theta_1 B(t) - \theta_2 S(t)}{\theta_1 V(t)} \right\}.$$

Taking all the aforementioned evidence into consideration, we arrive at the model below

$$\begin{aligned} S'(t) &= \alpha S - f(S)B, \\ V'(t) &= \gamma V \left[1 - \frac{V}{\min \left\{ K, \frac{N - \theta_1 B - \theta_2 S}{N_V} \right\}} \right] - g(V)B + \epsilon f(S)B + \psi B, \\ B'(t) &= e_1 f(S)B + e_2 \min \left\{ 1, \frac{N - \theta_1 B - \theta_2 S}{\theta_1 V} \right\} g(V)B - \lambda B, \end{aligned} \quad (2.2)$$

where the parameters are listed in Table 1.

In the following analysis, we assume a linear functional response for both predation of the salmon and the vegetation, i.e., $f(S) = \beta S$ and $g(V) = \delta V$. We analyze a special case where the element recycling for the vegetation is minimum and can be ignored, i.e., $\epsilon = 0$ and $\psi = 0$.

Table 1. Parameters of model (2.2).

Parameter	Description	Restrictions
α	Growth rate of salmon	$\alpha > 0$
β	Predation rate on salmon	$\beta > 0$
γ	Intrinsic growth rate for vegetation	$\gamma > 0$
K	Carrying capacity of vegetation limited by solar energy	$K > 0$
N	Total mass of nitrogen within the system	$N > 0$
θ_1	N: C ratio in bears	$\theta_1 > 0$
θ_2	N: C ratio in salmon	$\theta_2 > 0$
N_V	Minimum N:C ratio in vegetation	$N_V > 0$
δ	Predation rate on vegetation	$\delta > 0$
ϵ	Contribution to vegetation growth from dead salmon organ	$\epsilon \geq 0$
ψ	Contribution to vegetation growth from bear excretion	$\psi \geq 0$
e_1	Maximum biomass conversion efficiency via salmon consumption	$1 > e_1 > 0$
e_2	Maximum biomass conversion efficiency via vegetation consumption	$1 > e_2 > 0$
λ	Natural mortality rate of bears	$\lambda > 0$

In the following analysis, we restrict the positive invariant set Ω to be

$$\Omega = \{(S, V, B) : S > 0, V > 0, B > 0, \theta_1 B + \theta_2 S + N_V V < N\},$$

where the population densities are bounded by the total element concentration N in the ecosystem.

3. Mathematical analysis

3.1. Steady state solutions

We first analyze steady-state solutions of (2.2) when $\epsilon = 0, \psi = 0$. The steady-state solutions are determined by

$$\alpha S - \beta S B = 0, \quad (3.1)$$

$$\gamma V \left[1 - \frac{V}{\min\left\{K, \frac{N - \theta_1 B - \theta_2 S}{N_V}\right\}} \right] - \delta V B = 0, \quad (3.2)$$

$$e_1 \beta S B + e_2 \min\left\{1, \frac{N - \theta_1 B - \theta_2 S}{\theta_1 V}\right\} \delta V B - \lambda B = 0. \quad (3.3)$$

Here, (3.1) implies that $S = 0$ or $B = \alpha/\beta$. If salmon is at extinction, i.e., $S = 0$, then (3.3) implies that

$$B = 0 \quad \text{or} \quad e_2 \min\left\{1, \frac{N - \theta_1 B}{\theta_1 V}\right\} \delta V - \lambda = 0.$$

If the bear population is at extinction, i.e., $B = 0$, then (3.2) simplifies to

$$\gamma V \left[1 - \frac{V}{\min\{K, N/N_V\}} \right] = 0.$$

Therefore, we obtain an extinction equilibrium $E_0(0, 0, 0)$ and a vegetation-only equilibrium $E_1(0, \min\{K, N/N_V\}, 0)$ that always exist.

If

$$e_2 \min\left\{1, \frac{N - \theta_1 B}{\theta_1 V}\right\} \delta V - \lambda = 0,$$

then we have

$$V^* = \frac{\lambda}{e_2 \delta}, \quad \text{if} \quad \delta V \leq \frac{\delta}{\theta_1} (N - \theta_1 B), \quad (3.4)$$

or

$$\tilde{B} = \frac{N}{\theta_1} - \frac{\lambda}{e_2 \delta}, \quad \text{if} \quad \delta V > \frac{\delta}{\theta_1} (N - \theta_1 B). \quad (3.5)$$

When (3.4) holds, (3.2) reduces to

$$\gamma V^* \left[1 - \frac{V^*}{\min\left\{K, \frac{N - \theta_1 B}{N_V}\right\}} \right] - \delta V^* B = 0. \quad (3.6)$$

If $K < (N - \theta_1 B)/N_V$, then (3.6) leads to

$$B^* = \frac{\gamma}{\delta} \left(1 - \frac{V^*}{K} \right). \quad (3.7)$$

Therefore, a boundary equilibrium $E_2(0, V^*, B^*)$ exists if

$$\begin{cases} B^* < \min \left\{ \frac{N}{\theta_1} - \frac{\lambda}{e_2 \delta}, \frac{N}{\theta_1} - \frac{KN_V}{\theta_1} \right\}, \\ V^* < K. \end{cases} \quad (3.8)$$

If $K > (N - \theta_1 B)/N_V$, then (3.6) simplifies to

$$\gamma V^* - \frac{\gamma N_V (V^*)^2}{N - \theta_1 B} = \delta V^* B, \quad (3.9)$$

which is equivalent to

$$\Omega_1 B^2 + \Omega_2 B + \Omega_3 = 0,$$

where $\Omega_1 = \theta_1 \delta V^*$, $\Omega_2 = -V^*(\theta_1 \gamma + \delta N)$, $\Omega_3 = \gamma V^*(N - N_V V^*)$. By the invariant set Ω , we have $B < N/\theta_1$. We solve for B and reject the larger root to obtain

$$B^{**} = \frac{-\Omega_2 - \sqrt{\Omega_2^2 - 4\Omega_1\Omega_3}}{2\Omega_1}.$$

Therefore, a boundary equilibrium $E_3(0, V^*, B^{**})$ exists if

$$\frac{N}{\theta_1} - \frac{KN_V}{\theta_1} < B^{**} < \frac{N}{\theta_1} - \frac{\lambda}{e_2 \delta}.$$

Finally, when (3.5) holds, (3.2) reduces to

$$\gamma V \left[1 - \frac{V}{\min \left\{ K, \frac{N - \theta_1 \tilde{B}}{N_V} \right\}} \right] - \delta V \tilde{B} = 0. \quad (3.10)$$

Solving for V and rejecting the trivial solution leads to

$$\tilde{V} = \frac{\gamma - \delta \tilde{B}}{\gamma} \min \left\{ K, \frac{N - \theta_1 \tilde{B}}{N_V} \right\}.$$

Therefore, a boundary equilibrium $E_4(0, \tilde{V}, \tilde{B})$ exists if

$$\frac{N}{\theta_1} > \frac{\lambda}{e_2 \delta}, \quad \tilde{V} > \frac{\lambda}{e_2 \delta}.$$

Next, we analyze the existence of steady-state solutions when the bear population exists, i.e., $\hat{B} = \alpha/\beta$. Substituting \hat{B} into (3.3) gives

$$e_1 \beta \hat{B} S + e_2 \min \left\{ \delta \hat{B} V, \frac{\delta \hat{B}}{\theta_1} (N - \theta_1 \hat{B} - \theta_2 S) \right\} - \lambda \hat{B} = 0. \quad (3.11)$$

If $\delta\hat{B}V > [\delta\hat{B}(N - \theta_1\hat{B} - \theta_2S)]/\theta_1$, solving for S in (3.11) leads to

$$\bar{S} = \frac{\theta_1\lambda - e_2\delta(N - \theta_1\hat{B})}{e_1\beta\theta_1 - e_2\delta\theta_2}. \quad (3.12)$$

We further substitute \bar{S} into (3.2) and obtain

$$\gamma V \left[1 - \frac{V}{\min\{K, (N - \theta_1\hat{B} - \theta_2\bar{S})/N_V\}} \right] - \delta\hat{B}V = 0. \quad (3.13)$$

By solving for V and denoting the positive solution by \bar{V} , we obtain

$$\bar{V} = \min \left\{ K, \frac{N - \theta_1\hat{B} - \theta_2\bar{S}}{N_V} \right\} \left(1 - \frac{\delta\hat{B}}{\gamma} \right).$$

Therefore, a positive equilibrium $E_5(\bar{S}, \bar{V}, \hat{B})$ exists if

$$\frac{\theta_1\lambda - e_2\delta(N - \theta_1\hat{B})}{e_1\beta\theta_1 - e_2\delta\theta_2} > 0, \quad \bar{V} > \frac{N - \theta_1\hat{B} - \theta_2\bar{S}}{\theta_1}.$$

If $\delta\hat{B}V < [\delta\hat{B}(N - \theta_1\hat{B} - \theta_2S)]/\theta_1$, (3.3) simplifies to

$$e_1\beta S + e_2\delta V - \lambda = 0.$$

Solving for S gives

$$S = \frac{\lambda - e_2\delta V}{e_1\beta}. \quad (3.14)$$

We substitute (3.14) into (3.2) and obtain

$$\gamma V \left[1 - \frac{V}{\min\{K, [N - \theta_1\hat{B} - \theta_2(\lambda - e_2\delta V)/(e_1\beta)]/N_V\}} \right] - \delta\hat{B}V = 0. \quad (3.15)$$

If $K < (N - \theta_1\hat{B})/N_V - [\theta_2(\lambda - e_2\delta V)]/(e_1\beta N_V)$, or equivalently $[e_1\beta K N_V - (N - \theta_1\hat{B})e_1\beta + \lambda\theta_2]/[e_2\delta\theta_2] < V$, then (3.15) reduces to

$$\gamma V \left(1 - \frac{V}{K} \right) - \delta\hat{B}V = 0.$$

Solving for V and denoting the positive solution by \hat{V} gives

$$\hat{V} = \frac{K}{\gamma}(\gamma - \delta\hat{B}). \quad (3.16)$$

Therefore, a positive equilibrium $E_6(\hat{S}, \hat{V}, \hat{B})$ exists if

$$\begin{cases} (\theta_1 e_1 \beta - \theta_2 e_2 \delta) \hat{V} < e_1 \beta N - \theta_2 \lambda - \theta_1 e_1 \beta \hat{B}, \\ \hat{V} < \frac{\lambda}{e_2 \delta}, \quad \frac{e_1 \beta K N_V - (N - \theta_1 \hat{B}) e_1 \beta + \lambda \theta_2}{e_2 \delta \theta_2} < \hat{V}. \end{cases}$$

If $K > (N - \theta_1 \hat{B})/N_V - [\theta_2(\lambda - e_2 \delta V)]/(e_1 \beta N_V)$, or equivalently $V < [e_1 \beta K N_V - (N - \theta_1 \hat{B})e_1 \beta + \lambda \theta_2]/[e_2 \delta \theta_2]$, then (3.15) reduces to

$$\gamma V \left[1 - \frac{V}{(N - \theta_1 \hat{B})/N_V - \theta_2(\lambda - e_2 \delta V)/(e_1 \beta N_V)} \right] - \hat{B} \delta V = 0. \quad (3.17)$$

Solving for V and denoting the positive solution by V^+ leads to

$$V^+ = \frac{(\gamma - \hat{B} \delta) [e_1 \beta (N - \theta_1 \hat{B}) - \theta_2 \lambda]}{\gamma e_1 \beta N_V - (\gamma - \hat{B} \delta) \theta_2 e_2 \delta}.$$

Therefore, a positive equilibrium $E_7(S^+, V^+, \hat{B})$ exists if

$$\begin{cases} \theta_1 \hat{B} + \theta_2 S^+ + \theta_1 V^+ < N, \\ V^+ < \min \left\{ \frac{\lambda}{e_2 \delta}, \frac{e_1 \beta K N_V - (N - \theta_1 \hat{B})e_1 \beta + \lambda \theta_2}{e_2 \delta \theta_2} \right\}. \end{cases}$$

3.2. Stability of the steady-state solutions

Next, we analyze the local stability of the steady-state solutions. Direct calculations lead to the Jacobian matrix

$$J = \begin{pmatrix} \alpha - \beta B & 0 & -\beta S \\ J_{21} & J_{22} & J_{23} \\ J_{31} & J_{32} & J_{33} \end{pmatrix}, \quad (3.18)$$

where

$$\begin{aligned} J_{21} &= \begin{cases} 0, & \text{if } K < \frac{N - \theta_1 B - \theta_2 S}{N_V}, \\ -\frac{\gamma \theta_2 N_V V^2}{(N - \theta_1 B - \theta_2 S)^2}, & \text{if } K > \frac{N - \theta_1 B - \theta_2 S}{N_V}, \end{cases} \\ J_{22} &= \begin{cases} \gamma - \frac{2\gamma V}{K} - \delta B, & \text{if } K < \frac{N - \theta_1 B - \theta_2 S}{N_V}, \\ \gamma - \frac{2\gamma N_V V}{N - \theta_1 B - \theta_2 S} - \delta B, & \text{if } K > \frac{N - \theta_1 B - \theta_2 S}{N_V}, \end{cases} \\ J_{23} &= \begin{cases} -\delta V, & \text{if } K < \frac{N - \theta_1 B - \theta_2 S}{N_V}, \\ -\frac{\gamma \theta_1 N_V V^2}{(N - \theta_1 B - \theta_2 S)^2} - \delta V, & \text{if } K > \frac{N - \theta_1 B - \theta_2 S}{N_V}, \end{cases} \\ J_{31} &= \begin{cases} e_1 \beta B, & \text{if } 1 < \frac{N - \theta_1 B - \theta_2 S}{\theta_1 V}, \\ e_1 \beta B - \frac{e_2 \delta \theta_2}{\theta_1} B, & \text{if } 1 > \frac{N - \theta_1 B - \theta_2 S}{\theta_1 V}, \end{cases} \\ J_{32} &= \begin{cases} e_2 \delta B, & \text{if } 1 < \frac{N - \theta_1 B - \theta_2 S}{\theta_1 V}, \\ 0, & \text{if } 1 > \frac{N - \theta_1 B - \theta_2 S}{\theta_1 V}, \end{cases} \end{aligned}$$

$$J_{33} = \begin{cases} e_1\beta S + e_2\delta V - \lambda, & \text{if } 1 < \frac{N - \theta_1 B - \theta_2 S}{\theta_1 V}, \\ e_1\beta S + \frac{e_2\delta}{\theta_1}(N - 2\theta_1 B - \theta_2 S) - \lambda, & \text{if } 1 > \frac{N - \theta_1 B - \theta_2 S}{\theta_1 V}. \end{cases}$$

Then, the characteristic equation follows as $|\mu I - J| = 0$. By substituting each equilibrium into the characteristic equation, we are able to obtain the following theorems that state the stability results. The theorem below shows the stability of the bear-extinction equilibria.

Theorem 3.1. *The trivial equilibrium $E_0(0, 0, 0)$ and the vegetation-only equilibrium $E_1(0, \min\{K, N/N_V\}, 0)$ are unstable.*

Proof. By evaluating (3.18) at the trivial equilibrium E_0 and solving the characteristic equation $|\mu I - J| = 0$, we obtain the characteristic roots

$$\mu_1 = \alpha, \quad \mu_2 = \gamma, \quad \mu_3 = -\lambda,$$

which demonstrates that E_0 is unstable.

Similar calculations give the characteristic roots at E_1

$$\mu_1 = \alpha, \quad \mu_2 = -\gamma, \quad \mu_3 = \begin{cases} e_2\delta \min\left\{K, \frac{N}{N_V}\right\} - \lambda, & \text{if } \theta_1 \min\left\{K, \frac{N}{N_V}\right\} < N, \\ \frac{e_2\delta}{\theta_1}N - \lambda, & \text{if } \theta_1 \min\left\{K, \frac{N}{N_V}\right\} > N, \end{cases}$$

which shows that E_1 is unstable.

The following theorem shows the stability results of the salmon-extinction equilibria E_2, E_3, E_4 .

Theorem 3.2. *The salmon-extinction equilibrium E_2 is locally asymptotically stable if $\alpha/\beta < B^*$ and is unstable if otherwise. The salmon-extinction equilibrium E_3 is locally asymptotically stable if $\alpha/\beta < B^{**} < \gamma/\delta$ and is unstable if otherwise. The salmon-extinction equilibrium E_4 is locally asymptotically stable if $\alpha/\beta < \tilde{B} < \gamma/\delta$ and is unstable if otherwise.*

Proof. Direct calculations lead to the characteristic equation at E_2

$$(\mu - (\alpha - \beta B^*))(\mu^2 - J_{22}\mu - J_{23}J_{32}) = 0,$$

where $J_{22} = \gamma - (2\gamma V^*)/K - \delta B^*$, $J_{23} = -\delta V^*$, $J_{32} = e_2\delta B^*$. By using (3.7), we can simplify $J_{22} = \gamma - (2\gamma V^*)/K - \delta B^* = \gamma - (2\gamma V^*)/K - \gamma(1 - V^*/K) = -(\gamma V^*)/K < 0$. It follows that $\mu_1 = \alpha - \beta B^*$, $\mu_2 + \mu_3 = -(\gamma V^*)/K < 0$, $\mu_2\mu_3 = \delta V^* e_2\delta B^* > 0$. Therefore, E_2 is locally asymptotically stable if $\mu_1 < 0$, i.e., $(\alpha/\beta) < B^*$ and is unstable if otherwise.

Similarly, by evaluating (3.18) at E_3 , we obtain the characteristic equation at E_3

$$(\mu - (\alpha - \beta B^{**}))(\mu^2 - J_{22}\mu - J_{23}J_{32}) = 0,$$

where

$$J_{22} = \gamma - \frac{2\gamma N_V V^*}{N - \theta_1 B^{**}} - \delta B^{**}, \quad J_{23} = -\frac{\gamma \theta_1 N_V (V^*)^2}{(N - \theta_1 B^{**})^2} - \delta V^*,$$

$$J_{32} = e_2 \delta B^{**}.$$

This implies that $\mu_1 = \alpha - \beta B^{**}$, $\mu_2 + \mu_3 = J_{22}$, $\mu_2 \mu_3 = -J_{23} J_{32} > 0$. By using (3.9), we can further simplify $J_{22} = \gamma - 2(\gamma - \delta B^{**}) - \delta B^{**} = \delta B^{**} - \gamma$. Therefore, E_3 is locally asymptotically stable if $\mu_1 < 0$ and $\mu_2 + \mu_3 < 0$, which are equivalent to $\alpha/\beta < B^{**} < \gamma/\delta$.

Finally, direct calculations give the characteristic equation at E_4

$$(\mu - (\alpha - \beta \tilde{B}))(\mu - J_{22})(\mu - J_{33}) = 0,$$

where

$$J_{22} = \begin{cases} \gamma - \frac{2\gamma \tilde{V}}{K} - \delta \tilde{B}, & \text{if } K < \frac{N - \theta_1 B}{N_V}, \\ \gamma - \frac{2\gamma N_V \tilde{V}}{N - \theta_1 \tilde{B}} - \delta \tilde{B}, & \text{if } K > \frac{N - \theta_1 B}{N_V}, \end{cases}$$

$$J_{33} = \lambda - \frac{e_2 \delta N}{\theta_1}.$$

We can further simplify J_{22} by using (3.10) to obtain $J_{22} = \delta \tilde{B} - \gamma$. Moreover, $J_{33} < 0$ is satisfied automatically when E_4 exists. Therefore, E_4 is locally asymptotically stable if $\alpha/\beta < \tilde{B} < \gamma/\delta$ and is unstable otherwise.

Finally, the following theorem shows the local stabilities of the positive equilibria E_5, E_6, E_7 .

Theorem 3.3. *The positive equilibrium $E_5(\bar{S}, \bar{V}, \hat{B})$ is locally asymptotically stable if $e_1 \beta \theta_1 > e_2 \delta \theta_2$ and is unstable if otherwise. The positive equilibrium $E_6(\hat{S}, \hat{V}, \hat{B})$ is locally asymptotically stable if*

$$\frac{e_2 \delta (\delta - \beta) K (\gamma - \delta \hat{B})}{\gamma} + \beta \lambda > 0$$

and is unstable if otherwise. The positive equilibrium $E_7(S^+, V^+, \hat{B})$ is always unstable.

Proof. Direct calculations give the characteristic equation at E_5

$$(\mu - J_{22})(\mu^2 - J_{33}\mu - J_{13}J_{31}) = 0,$$

where

$$J_{22} = \begin{cases} \gamma - \frac{2\gamma \bar{V}}{K} - \delta \hat{B}, & \text{if } K < \frac{N - \theta_1 \hat{B} - \theta_2 \bar{S}}{N_V}, \\ \gamma - \frac{2\gamma N_V \bar{V}}{N - \theta_1 \hat{B} - \theta_2 \bar{S}} - \delta \hat{B}, & \text{if } K > \frac{N - \theta_1 \hat{B} - \theta_2 \bar{S}}{N_V}, \end{cases}$$

$$J_{33} = e_1 \beta \bar{S} + \frac{e_2 \delta}{\theta_1} (N - 2\theta_1 \hat{B} - \theta_2 \bar{S}) - \lambda,$$

$$J_{13} = -\beta \bar{S}, \quad J_{31} = \hat{B} \frac{e_1 \beta \theta_1 - e_2 \delta \theta_2}{\theta_1}.$$

By using (3.12), we can simplify J_{33} as $J_{33} = -e_2\delta\hat{B} < 0$. Moreover, by using (3.13), we can simplify J_{22} to

$$J_{22} = \begin{cases} -\frac{\gamma\bar{V}}{K} < 0, & \text{if } K < \frac{N - \theta_1\hat{B} - \theta_2\bar{S}}{N_V}, \\ -\frac{\gamma N_V\bar{V}}{N - \theta_1\hat{B} - \theta_2\bar{S}} < 0, & \text{if } K > \frac{N - \theta_1\hat{B} - \theta_2\bar{S}}{N_V}. \end{cases}$$

The above analyses show that E_5 is locally asymptotically stable if $J_{31} > 0$ or equivalently $e_1\beta\theta_1 > e_2\delta\theta_2$.

Similarly, by evaluating (3.18) at E_6 , we obtain the characteristic equation

$$\mu^3 - (J_{22} + J_{33})\mu^2 + (J_{22}J_{33} - J_{23}J_{32} - J_{13}J_{31})\mu + J_{13}J_{31}J_{22} = 0,$$

where

$$\begin{aligned} J_{13} &= -\beta\hat{S} < 0, & J_{22} &= \gamma - \frac{2\gamma\hat{V}}{K} - \delta\hat{B}, & J_{23} &= -\delta\hat{V} < 0, \\ J_{31} &= e_1\beta\hat{B} > 0, & J_{32} &= e_2\delta\hat{B} > 0, & J_{33} &= e_1\beta\hat{S} + e_2\delta\hat{V} - \lambda. \end{aligned}$$

By the Routh-Hurwitz stability criterion, E_6 is locally asymptotically stable if

$$\begin{cases} -(J_{22} + J_{33}) > 0, \\ J_{22}J_{33} - J_{23}J_{32} - J_{13}J_{31} > 0, \\ J_{13}J_{31}J_{22} > 0, \\ -(J_{22} + J_{33})(J_{22}J_{33} - J_{23}J_{32} - J_{13}J_{31}) > J_{13}J_{31}J_{22}. \end{cases} \quad (3.19)$$

Here we can simplify J_{22} and J_{33} by using (3.16) and (3.14) respectively to obtain

$$J_{22} = -\frac{\gamma\hat{V}}{K} < 0, \quad J_{33} = 0,$$

which further reduce (3.19) to

$$\begin{cases} -J_{22} > 0, \\ J_{23}J_{32} + J_{13}J_{31} < 0, \\ J_{13}J_{31}J_{22} > 0, \\ J_{22}J_{23}J_{32} > 0. \end{cases}$$

Therefore, E_6 is locally asymptotically stable if $J_{23}J_{32} + J_{13}J_{31} < 0$ or equivalently

$$\frac{e_2\delta(\delta - \beta)K(\gamma - \delta\hat{B})}{\gamma} + \beta\lambda > 0.$$

Finally, similar to the above analyses, we obtain the characteristic equation at E_7

$$\mu^3 - J_{22}\mu^2 - (J_{23}J_{32} + J_{13}J_{31})\mu + J_{13}(J_{31}J_{22} - J_{21}J_{32}) = 0,$$

where

$$\begin{aligned} J_{13} &= -\beta S^+ < 0, & J_{21} &= -\frac{\gamma\theta_2 N_V V^2}{(N - \theta_1 B - \theta_2 S)^2} < 0, \\ J_{22} &= \gamma - \frac{2\gamma N_V V}{N - \theta_1 B - \theta_2 S} - \delta B, & J_{23} &= -\frac{\gamma\theta_1 N_V V^2}{(N - \theta_1 B - \theta_2 S)^2} - \delta V < 0, \\ J_{31} &= e_1\beta\hat{B} > 0, & J_{32} &= e_2\delta\hat{B} > 0, & J_{33} &= e_1\beta S^+ + e_2\delta V^+ - \lambda. \end{aligned}$$

By the Routh-Hurwitz criterion, E_7 is locally asymptotically stable if

$$\begin{cases} -J_{22} > 0, \\ -(J_{23}J_{32} + J_{13}J_{31}) > 0, \\ J_{13}(J_{31}J_{22} - J_{21}J_{32}) > 0, \\ J_{22}(J_{23}J_{32} + J_{13}J_{31}) > J_{13}(J_{31}J_{22} - J_{21}J_{32}). \end{cases}$$

Here it is obvious that $-(J_{23}J_{32} + J_{13}J_{31}) > 0$. Next, by substituting (3.14) and (3.17) into J_{22} , we can simplify

$$\begin{aligned} J_{22} &= \gamma - \frac{2\gamma N_V V}{N - \theta_1 B - \theta_2 S} - \delta B \\ &= \frac{e_1 \beta N_V \gamma V}{e_1 \beta N - e_1 \beta \theta_1 \hat{B} - \theta_2 \lambda + \theta_2 e_2 \delta V} - \frac{2\gamma N_V V}{N - \theta_1 \hat{B} - \theta_2 S} < 0, \end{aligned}$$

which is satisfied when E_7 exists. Moreover, $J_{22}(J_{23}J_{32} + J_{13}J_{31}) > J_{13}(J_{31}J_{22} - J_{21}J_{32})$ is equivalent to $J_{22}J_{23} + J_{13}J_{21} > 0$. It remains to verify that $J_{13}(J_{31}J_{22} - J_{21}J_{32}) > 0$ or equivalently $J_{31}J_{22} - J_{21}J_{32} < 0$. Here $J_{31}J_{22} - J_{21}J_{32} < 0$ can be simplified to $0 < -\gamma\theta_2 N_V e_2 \delta V^2$ by substituting (3.14) and (3.17), which leads to the contradiction. Therefore, E_7 is always unstable when exists. Thus, completes the proof.

4. Numerical simulations

4.1. Simulation of (2.2) with a linear predation

Now we explore the dynamics of (2.2) numerically. For the numerical simulation, we will be assuming that the salmon-bear-vegetation ecological system lies within the riparian forests of Alaska. More specifically, we will be looking at a 100km² region of Lynx Creek, a tributary of the Wood River Lakes system in the Bristol Bay region of southwestern Alaska, USA (59°29'N, 158°55'W) [2]. This is a well-documented region where we will be able to get accurate values for our parameters. Based on data from [2], we explore the following scenarios by using biologically realistic parameters.

Figure 1 shows that the salmon-extinction boundary equilibrium is locally asymptotically stable. In particular, 1(a) demonstrates that E_2 is locally asymptotically stable, whereas both E_3, E_4 do not exist under the parameter set. Figure 1(b) indicates that E_3 is locally asymptotically stable, whereas both E_2, E_4 do not exist under the parameter set. Moreover, Figure 1(c) shows that E_4 is locally asymptotically stable, whereas both E_2, E_3 do not exist under the parameter set. Via our extensive numerical experiments, we find that E_2 cannot coexist with either/both E_3, E_4 .

Figure 2 demonstrates that all salmon, vegetation and bear populations coexist together. Figure 2(a) shows that the positive equilibrium E_5 is locally asymptotically stable, whereas E_6 does not exist under the parameter set. Figure 2(b) shows that the positive equilibrium E_6 is locally asymptotically stable, whereas E_5 does not exist under the parameter set.

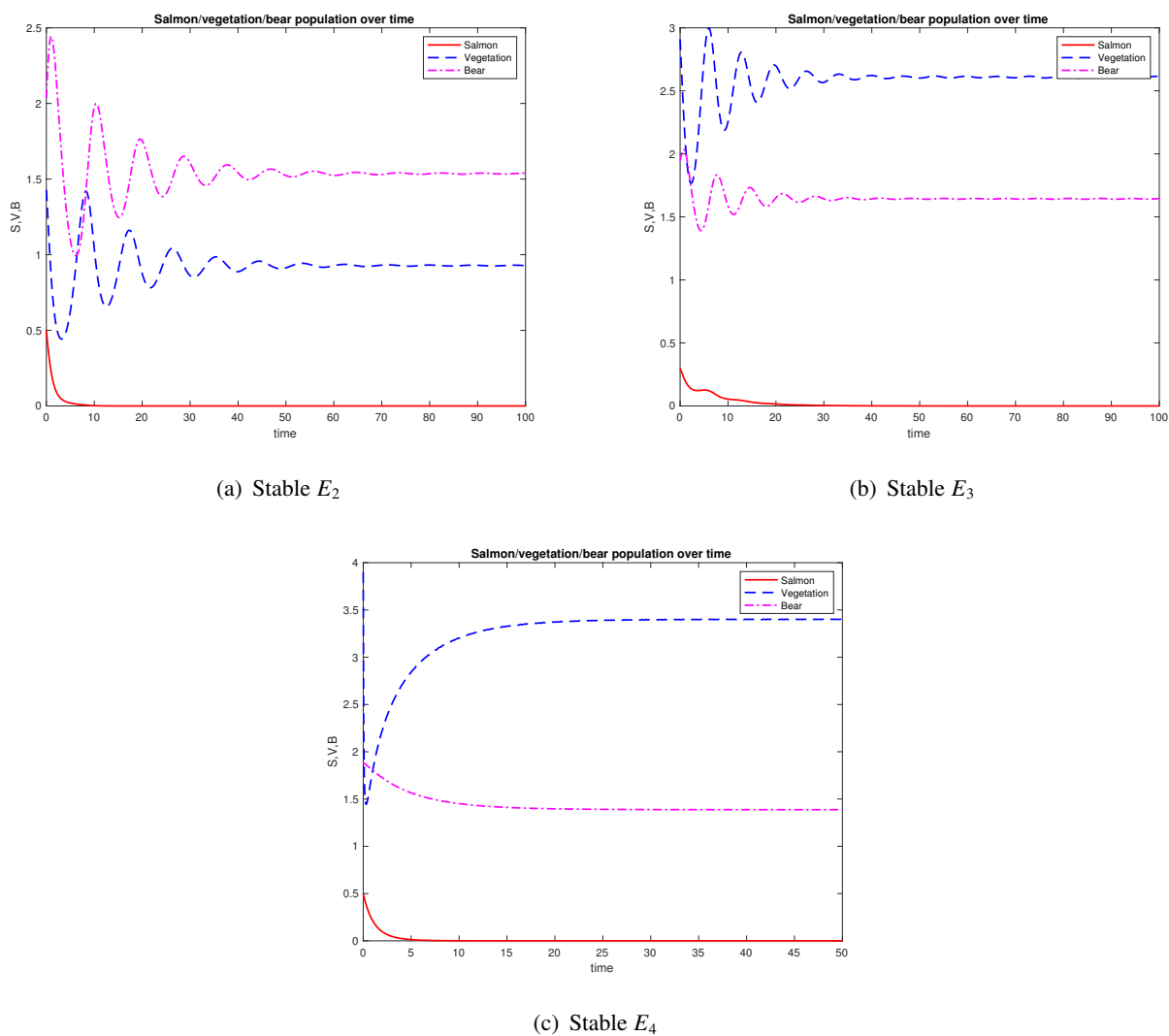


Figure 1. Locally asymptotically stable E_2, E_3, E_4 respectively. Parameter values for 1(a): $\alpha = 0.008, \beta = 0.3507, \gamma = 1.1036, K = 6.8951, N = 0.9533, \theta_1 = 0.2371, \theta_2 = 0.1371, N_V = 0.0115, \delta = 0.6217, e_1 = 0.5676, e_2 = 0.8817, \lambda = 0.5088$. Parameter values for 1(b): $\alpha = 0.9746, \beta = 0.6764, \gamma = 1.4623, K = 35.4971, N = 0.9610, \theta_1 = 0.2046, \theta_2 = 0.1046, N_V = 0.0367, \delta = 0.7535, e_1 = 0.4830, e_2 = 0.3214, \lambda = 0.6319$. Parameter values for 1(c): $\alpha = 0.8815, \beta = 0.9483, \gamma = 9.7637, K = 33.1267, N = 0.6990, \theta_1 = 0.2623, \theta_2 = 0.1623, N_V = 0.0873, \delta = 0.8055, e_1 = 0.1425, e_2 = 0.1705, \lambda = 0.1755$.

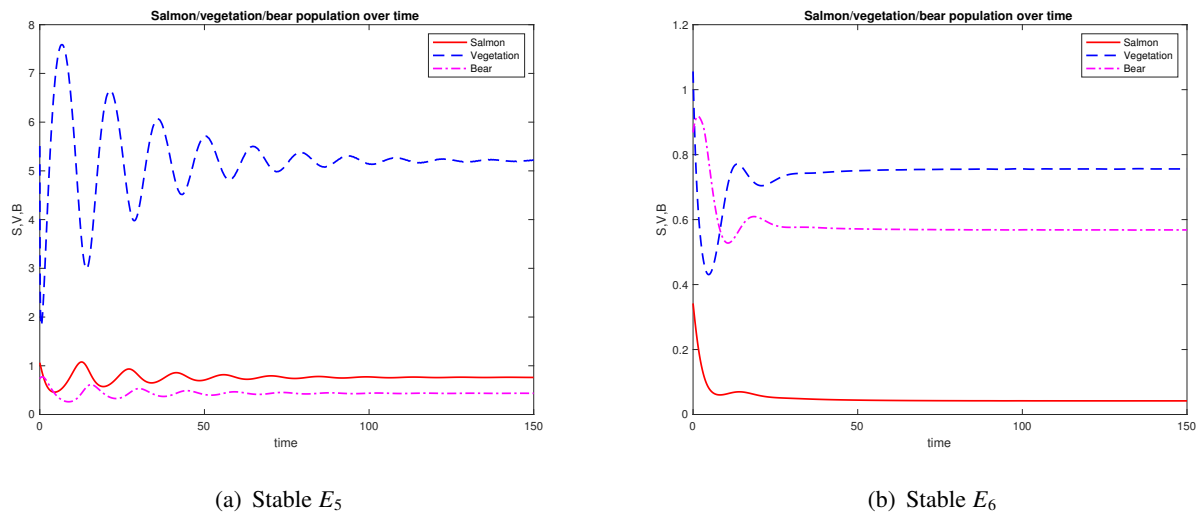


Figure 2. Locally asymptotically stable E_5, E_6 respectively. Parameter values for 2(a): $\alpha = 0.3860, \beta = 0.8874, \gamma = 4.7299, K = 18.1625, N = 0.9595, \theta_1 = 0.5330, \theta_2 = 0.4330, N_V = 0.0720, \delta = 0.6159, e_1 = 0.8917, e_2 = 0.2849, \lambda = 0.7341$. Parameter values for 2(b): $\alpha = 0.5441, \beta = 0.9575, \gamma = 0.9652, K = 1.6234, N = 0.9988, \theta_1 = 0.6647, \theta_2 = 0.5647, N_V = 0.0758, \delta = 0.9076, e_1 = 0.8909, e_2 = 0.4548, \lambda = 0.3478$.

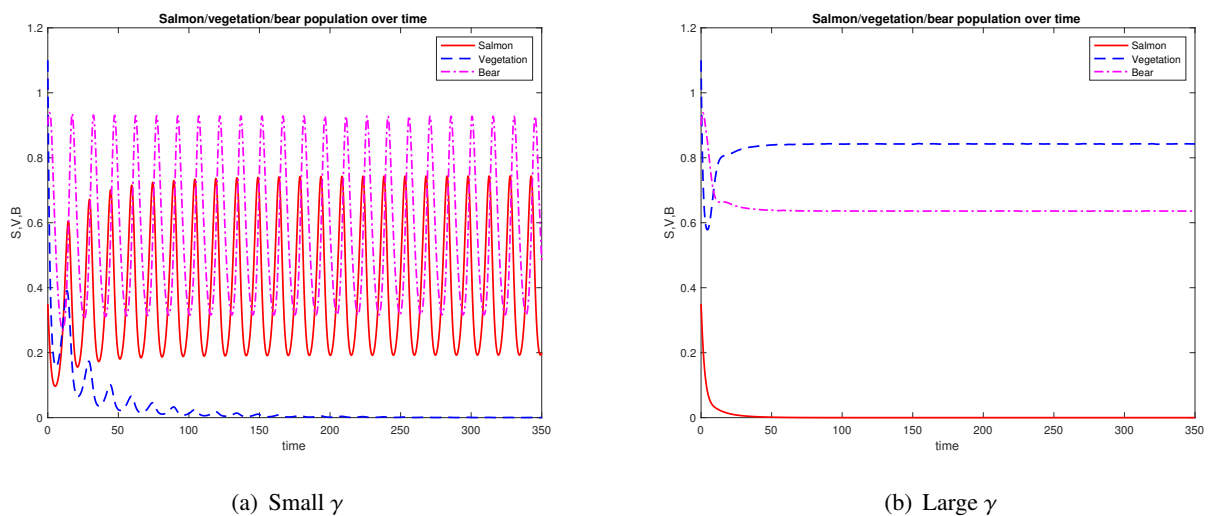


Figure 3. Salmon, vegetation and bear populations over time with small γ (3(a)) or large γ (3(b)). The parameters are the same as Figure 2(b) except γ , where $\gamma = 0.5$ for 3(a) and $\gamma = 1.2$ for 3(b).

Next, we explore how the vegetation growth rate impacts the long-term dynamics of (2.2). We generate Figure 3 by using the same set of parameter as Figure 2(b) but varying γ . Figure 3(a) demonstrates that a small vegetation growth rate drives the vegetation population to extinction, whereas salmon co-exist with bears, but the populations oscillate periodically. On the other hand, the salmon population

goes to extinction, but the vegetation coexists with bears at a steady state when γ is large. The results are reasonable biologically because a small vegetation growth rate cannot sustain the persistence of the vegetation population. However, a large vegetation growth rate facilitates the nitrogen recycling of the vegetation, which supports the bear population via consumption but drives the salmon population to extinction due to the scarcity of nitrogen.

Finally, Figure 4(a) demonstrates another scenario where the salmon, bear and vegetation coexist but the populations oscillate periodically. However, Figure 4(b) shows that a larger vegetation growth rate may stabilize the oscillating populations to a steady state.

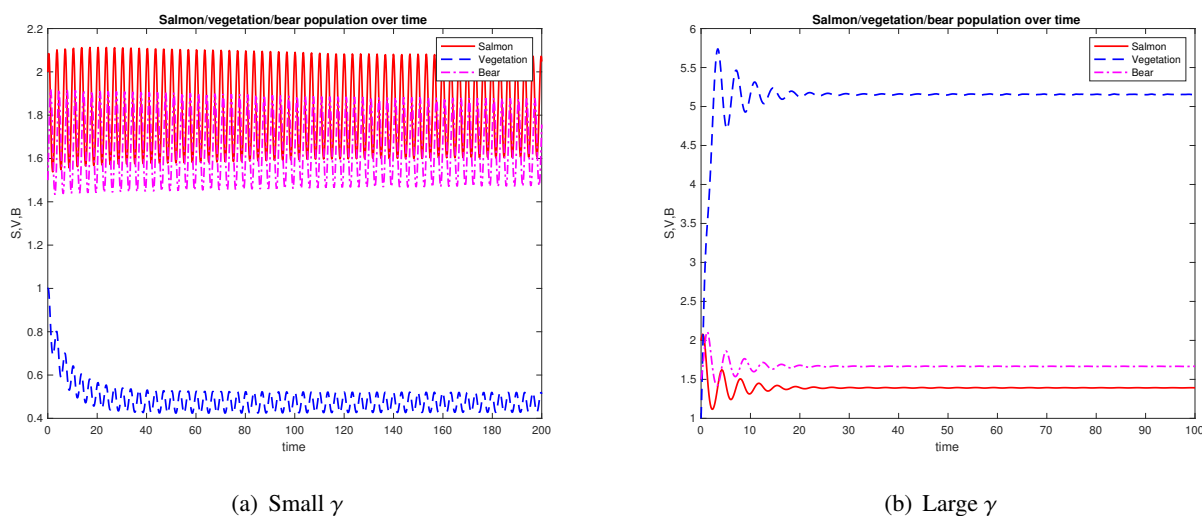


Figure 4. Salmon, vegetation and bear populations over time with small γ (4(a)) or large γ (4(b)). The parameters values are $\alpha = 2, \beta = 1.2, K = 15, N = 1.2, \theta_1 = 0.1, \theta_2 = 0.15, N_V = 0.1, \delta = 0.9, e_1 = 0.8, e_2 = 0.1, \lambda = 1.8, \gamma = 1.6$ for 4(a), and $\gamma = 4$ for 4(b).

4.2. Simulation of (2.2) with a logistic growth of the salmon population and Holling type II predation

Next, we explore the extended model of (2.2) where the salmon population follows a logistic growth

$$S'(t) = \alpha S \left(1 - \frac{S}{K_1} \right) - f(S)B.$$

We consider that the predation of the salmon and the vegetation now follow the Holling type II functional response [15]

$$f(S) = \frac{\beta S}{h_1 + S}, \quad g(V) = \frac{\delta V}{h_2 + V},$$

where h_1, h_2 represent the half-saturating constants respectively.

Figure 5(a) demonstrates the bifurcation diagram of the salmon population with respect to the salmon carrying capacity K_1 . Moreover, Figure 5(b) demonstrates the bifurcation diagram of the vegetation population with respect to K_1 . The bifurcation diagram of the bear population with respect to K_1 is similar to Figure 5(a) and is thus omitted. Figure 5 shows that the salmon, vegetation and bear populations coexist at a steady state if the salmon carrying capacity is relatively small. However, when K_1

increases and passes 4.1, the vegetation population goes to extinction, whereas the salmon population coexists with the bear population at a steady state. Moreover, when K_1 further increases and passes 5.7, the vegetation population remains at extinction, but the salmon and bear populations oscillate periodically. The results are biologically reasonable because if the salmon carrying capacity is relatively small, the salmon, vegetation and bear compete for the nutrients but coexist due to the scarcity of the salmon population. However, if the salmon carrying capacity is at the intermediate range, the competition for nutrients drives the vegetation population to extinction because the salmon and bear are more nutrient-rich. Finally, a large salmon carrying capacity destabilizes the coexistence steady-state of the salmon and bear due to the enrichment of salmon.

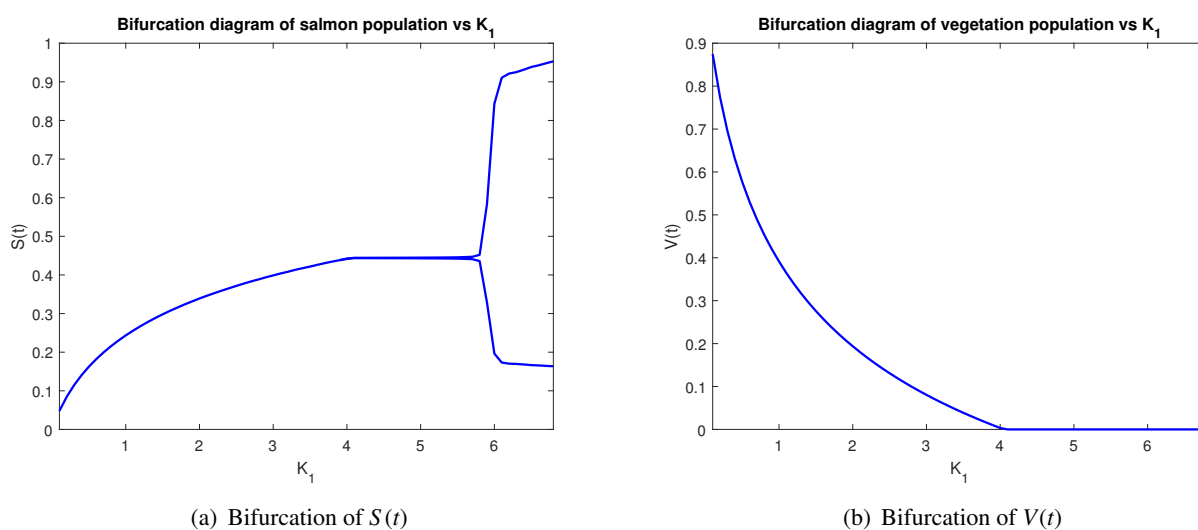


Figure 5. Bifurcation diagram of the salmon population/vegetation population with respect to the salmon carrying capacity K_1 for 5(a) and 5(b) respectively. The parameters values are the same as 3(a) except $\beta = 4.7875$, $\delta = 4.538$, $h_1 = 5$, $h_2 = 5$.

Next, to compare the dynamics of the salmon-vegetation-bear model with the grazer-consumer model in [6], we run the simulation by using the same set of parameters as in [6], except the salmon carrying capacity K_1 and the half-saturating constant of the salmon consumption h_1 . Figure 6 shows the bifurcation diagram of the salmon population/vegetation population/bear population with respect to the vegetation carrying capacity K respectively. If K is relatively small, Figure 6 shows that the salmon, bear and vegetation populations coexist at a steady state. However, when K increases and passes 0.24, the salmon population goes to extinction, whereas the vegetation and bear populations coexist at a steady state. If K further increases and passes 0.55, the vegetation and bear coexist but the populations oscillate periodically. If K further increases and passes 0.97, the vegetation and bear populations coexist but return to the steady state status. Finally, if K becomes relatively large and passes 1.5, the salmon population is no longer extinct but coexists with the vegetation and bear populations at a steady state.

Overall, when K is within the intermediate range, i.e., the salmon population is at extinction, Figures 6(a), 6(b) and 6(c) demonstrate similar dynamics with the producer-grazer model in [6]. The vegetation-bear coexistent steady state loses stability due to energy enrichment. However, a larger car-

rying capacity limited by the light energy drives the oscillating vegetation and bear populations to a steady state because of the competition for nutrients. Different from the results in [6], the bear population does not go to extinction but coexists with either/both salmon or/and vegetation populations when K is relatively small or large. The results suggest that a low or high carrying capacity limited by light energy facilitates the persistence of all salmon, vegetation and bear populations. Moreover, an intermediate carrying capacity limited by light energy drives the salmon population to extinction.

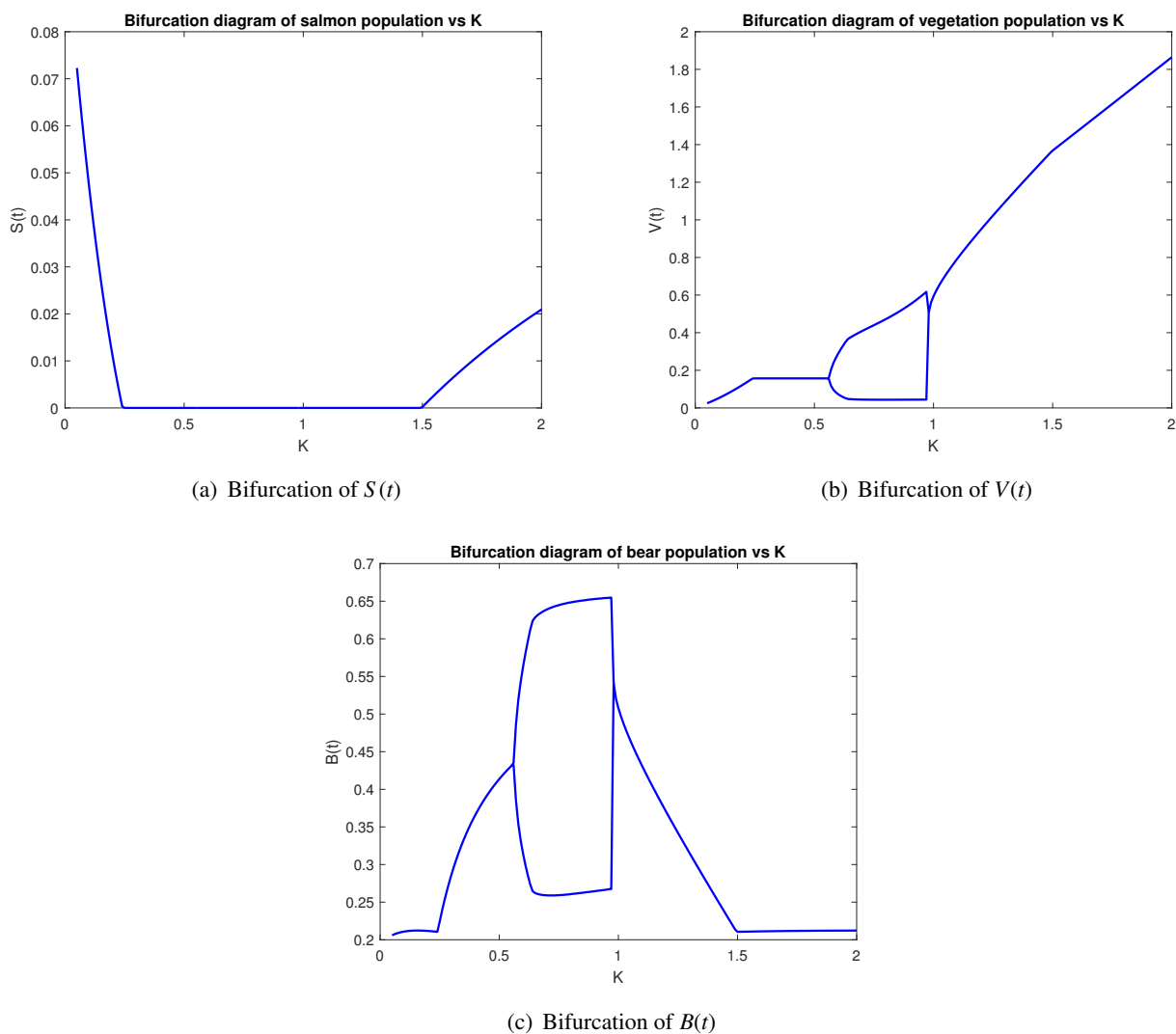


Figure 6. Bifurcation diagram of the salmon population/vegetation population/bear population with respect to the vegetation carrying capacity K for 6(a), 6(b) and 6(c) respectively. Parameters values: $\alpha = 0.8, \beta = 0.95, \gamma = 1.2, N = 0.025, \theta_1 = 0.03, \theta_2 = 0.03, N_V = 0.0038, \delta = 0.81, e_1 = 0.9, e_2 = 0.8, \lambda = 0.25, K_1 = 0.3, h_1 = 0.25, h_2 = 0.25$.

5. Conclusions and discussion

In this paper, we study an ecosystem of bears, salmon and vegetation, where bears consume salmon and vegetation for survival. Because salmon return to their natal streams to spawn and carry marine-derived nutrients, it is important to characterize the nutritional level difference between salmon, bears, and vegetation. In general, salmon and bears are more nutrient-rich compared to vegetation but must maintain homeostasis of the nutritional level within their bodies. On the other side, vegetation is less nutrient-rich but can recycle the remaining nutrient in the environment and the nutritional level within the body may differ significantly.

We propose a stoichiometric predator-prey model that tracks both the energy flow and the nutrient recycling from one trophic level to another. Analytical results show that boundary equilibria E_0, E_1 where bears are extinct exist but are always unstable. Moreover, boundary equilibria E_2, E_3, E_4 where salmon are extinct but bears persist may exist and remain locally asymptotically stable if certain conditions are satisfied. Positive equilibria E_5, E_6, E_7 where salmon, bears and vegetation coexist may exist if certain conditions are satisfied. Analyses show that E_5 and E_6 may remain locally asymptotically stable under certain conditions, but E_7 is always unstable.

Numerical simulations demonstrate that a small vegetation growth rate may drive the vegetation population to extinction where the salmon population and the bear population coexist in the periodic setting. Moreover, a large vegetation growth rate may drive the salmon population to extinction but the vegetation coexists with the bears at a steady state. Alternatively, the salmon, bears and vegetation populations may coexist periodically. In this scenario, a large vegetation growth rate may stabilize the system and drive the salmon, bear and vegetation to coexist at a steady state.

In this paper, for the analytical analysis, we adopt the linear functional response for the predation of the salmon and the predation of the vegetation in (2.2) for simplicity. However, a linear functional response has its limitation and is more suitable for an ecosystem with a sparse population density. A Holling type II functional response has a saturating effect when population density becomes large and therefore may be suitable for a broader regime [15]. Figures 5 and 6 in the simulation also confirm that rich dynamics may occur if the Holling type II functional response is adopted. Because of the nonlinearity of the Holling type II functional response, we expect that the analytical analysis becomes more challenging but on the other hand may deepen our understanding of the ecosystem of keystone species, which leaves as future works.

Use of AI tools declaration

The authors declare they have not used Artificial Intelligence (AI) tools in the creation of this article.

Acknowledgments

CM is grateful for funding from the NSERC USRA. XW is grateful for funding from the NSERC of Canada (RGPIN-2020-06825 and DGEER-2020-00369).

Conflict of interest

The authors declare there is no conflict of interest.

References

1. R. T. Paine, A conversation on refining the concept of keystone species, *Conserv. Biol.*, **9** (1995), 962–964. <https://doi.org/10.1046/j.1523-1739.1995.09040962.x>
2. J. M. Helfield, R. J. Naiman, Keystone interactions: salmon and bear in riparian forests of Alaska, *Ecosystems*, **9** (2006), 167–180. <https://doi.org/10.1007/s10021-004-0063-5>
3. T. Andersen, J. J. Elser, D. O. Hessen, Stoichiometry and population dynamics, *Ecol. Lett.*, **7** (2004), 884–900. <https://doi.org/10.1111/j.1461-0248.2004.00646.x>
4. J. J. Elser, W. F. Fagan, R. F. Denno, D. R. Dobberfuhl, A. Folarin, A. Huberty, et al., Nutritional constraints in terrestrial and freshwater food webs, *Nature*, **408** (2000), 578–580. <https://doi.org/10.1038/35046058>
5. E. B. Muller, R. M. Nisbet, S. A. Kooijman, J. J. Elser, E. McCauley, Stoichiometric food quality and herbivore dynamics, *Ecol. Lett.*, **4** (2001), 519–529. <https://doi.org/10.1046/j.1461-0248.2001.00240.x>
6. I. Loladze, Y. Kuang, Stoichiometry in producer-grazer systems: linking energy flow with element cycling, *Bull. Math. Biol.*, **62** (2000), 1137–1162. <https://doi.org/10.1006/bulm.2000.0201>
7. M. Chen, M. Fan, Y. Kuang, Global dynamics in a stoichiometric food chain model with two limiting nutrients, *Math. Biosci.*, **289** (2017), 9–19. <https://doi.org/10.1016/j.mbs.2017.04.004>
8. X. Li, H. Wang, Y. Kuang, Global analysis of a stoichiometric producer-grazer model with Holling-type functional responses, *J. Math. Biol.*, **63** (2011), 901–932. <https://doi.org/10.1007/s00285-010-0392-2>
9. I. Loladze, Y. Kuang, J. J. Elser, W. F. Fagan, Competition and stoichiometry: coexistence of two predators on one prey, *Theor. Popul. Biol.*, **65** (2004), 1–15. [https://doi.org/10.1016/S0040-5809\(03\)00105-9](https://doi.org/10.1016/S0040-5809(03)00105-9)
10. A. Peace, H. Wang, Y. Kuang, Dynamics of a producer-grazer model incorporating the effects of excess food nutrient content on grazer's growth, *Bull. Math. Biol.*, **76** (2014), 2175–2197. <https://doi.org/10.1007/s11538-014-0006-z>
11. H. Stech, B. Peckham, J. Pastor, Enrichment in a general class of stoichiometric producer-consumer population growth models, *Theor. Popul. Biol.*, **81** (2012), 210–222. <https://doi.org/10.1016/j.tpb.2012.01.003>
12. H. Wang, Y. Kuang, I. Loladze, Dynamics of a mechanistically derived stoichiometric producer-grazer model, *J. Biol. Dyn.*, **2** (2008), 286–296. <https://doi.org/10.1080/17513750701769881>
13. T. Xie, X. Yang, X. Li, H. Wang, Complete global and bifurcation analysis of a stoichiometric predator-prey model, *J. Dyn. Differ. Equations*, **30** (2018), 447–472. <https://doi.org/10.1007/s10884-016-9551-5>

14. T. Phan, J. J. Elser, Y. Kuang, Rich dynamics of a general producer-grazer interaction model under shared multiple resource limitations, *Appl. Sci.*, **13** (2023), 4150. <https://doi.org/10.3390/app13074150>
15. C. S. Holling, The functional response of predators to prey density and its role in mimicry and population regulation, *The Memoirs of the Entomological Society of Canada*, **97** (1965), 5–60. <https://doi.org/10.4039/entm9745fv>



AIMS Press

©2023 the Author(s), licensee AIMS Press. This is an open access article distributed under the terms of the Creative Commons Attribution License (<http://creativecommons.org/licenses/by/4.0>)